An Integrated Approach for Perfusion Lesion Segmentation using MR Perfusion for Acute Ischemic Stroke

D. D. Shanbhag[1], R. Mullick[1], S. K. Nath[1], C. Oppenheim[2], M. Luby[3], K. D. Ku[3], L. L. Latour[3], S. Warach[3], and . NINDS Natural History of Stroke Investigators[3]

[1]Imaging Technologies, GE Global Research, Bangalore, Karnataka, India, [2]Department of Neuroradiology, Université Paris-Descartes, Paris, France, [3]NINDS, NIH, Bethesda, MD, United States

Introduction: One of the goals of MR imaging in acute ischemic stroke (AIS) is to identify tissue, which can be salvaged with reperfusion therapies. The salvageable tissue with MRI is approximated as regions of perfusion change without a corresponding diffusion abnormality and termed as the diffusion–perfusion mismatch [1]. Though the ease of its measurement has made mismatch (MM) an attractive candidate for therapeutic decisions in clinical settings, its routine use is hindered by the long time needed to mark the PWI lesion [2]. We have developed a mismatch calculator tool based on fast and reliable segmentation of DWI and PWI lesions. Previous work in this area has focused on using a supervised approach mismatch calculation [3] or automated workflow using a particular type of PWI quantitative map [4]. In this work, we correlate our automated mismatch segmentation across different PWI maps (MTT, T_{max}, TTP) with retrospective manual analysis and demonstrate its use in AIS.

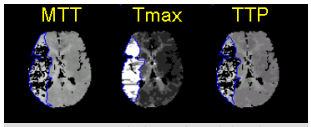

Figure 1. Use of clustering, island statistics and DWI feedback results in reliable PWI lesion segmentation (MTT lesion = 255 cc, Tmax lesion = 215 cc and TTP lesion = 224 cc)

Methods and Materials: ***Patient database:*** Data for our study was acquired from 2000-2008, from patients treated with standard IV-tPA after a baseline, pre-treatment MRI at multiple centers. The appropriate IRBs approved the studies. We segregated our database into two sets, one for which the ground-truth (GT): DWI and PWI lesion markings were available (Set#1, N = 25) and other for which no GT was done (Set #2, N= 59). ***Imaging:*** All MRI datasets were acquired on a 1.5T GE Signa Genesis and GE Signa HDx clinical scanners using an 8-channel head or NV coil. (a) DWI imaging: Axial DWI trace images were acquired using a SE-EPI sequence, TE=67–100 ms, TR=4.5–7s, FA=90°, NEX=2, 256x256 matrix, FOV = 240x240 mm^2, slice thickness = 3.5-7 mm, b = 0 s/mm^2 and 1000 s/mm^2. (b) PWI Imaging: Axial oblique slices were acquired using a GE-EPI sequence, TE = 19–60 ms, TR = 1000–2275 ms, FA = 90°, number of phase measurements varying from 25 (2 s/phase) to 100 (1s/phase), slice thickness = 5–7mm, Matrix: 64 x 64 -128 x 128, FOV = 240x 240 mm^2. ***PWI Map generation:*** The tool calculated maps used for PWI lesion segmentation. To avoid the EPI ghosts from affecting the PWI lesion segmentation, skull removal was done using the non-saturated PWI phase volume and applied to all bolus phase volumes. Following the skull strip, volumes were aligned along the mid-sagittal plane (MSP) for contralateral analysis [5]. For each PWI dataset, a global bolus arrival time (BAT) was determined by using a threshold based on the entire ensemble of signal curves and MTT and TTP calculation were referenced to it. For each concentration curve, a recirculation cutoff was determined and MTT map calculated between global BAT and cutoff. Time to peak (TTP) was defined as the time between the global BAT and curve peak. AIF and VOF were selected automatically by the program and used to generate the T_{max} maps [6]. All indeterminate values were flagged and used in further analysis. ***Image Analysis:*** (a) *Registration:* PWI data was co-registered to DWI data and facilitated cross talk between the two channels of information. (b) *PWI segmentation:* Perfusion lesion segmentation is based on contralateral difference analysis of MSP corrected; skull stripped quantitative maps and uses feedback from the co-registered DWI and ADC maps. For each map, regional statistics (mean, SD, median, percentiles) was obtained and used to determine the PWI lesion location and an optimal difference threshold for contralateral analysis. Optimal threshold calculation also took into account the discrete nature of T_{max} maps. Alternatively user could provide a fixed difference threshold for analysis. To account for differences in symmetry of the brain, a neighborhood kernel was used to decide if the tissue was part of PWI lesion or not. Tissue was part of perfusion lesion if its neighborhood statistics were greater than the optimal threshold or if the tissue quantitative map had indeterminate values. Post contralateral analysis, a clustering algorithm was used to collate the disjoint islands into single lesion and reject the noise islands. The settings of clustering algorithm were varied depending on the morphology and statistics of the islands. Following the clustering, the final PWI lesion was obtained by removing the ventricles (using the registered ADC map) from the clustered mask, and generic hole filling. (c) *Mismatch:* Mismatch between the DWI and PWI lesions was calculated as follows: MM=PWI_lesion–(PWI_lesion∩DWI_lesion). All the parameters for map generation and image analysis could be easily changed through a flexible xml-based configuration file. The entire pipeline (MSP, map generation, registration, segmentation and mismatch) was implemented using the functionality available in the Insight Toolkit (ITK) [7]. (d) *GT generation and evaluation:* A trained imaging scientist marked lesion locations on DWI images and MTT maps, smoothened and interpolated to match DWI matrix size, which formed the ground truth [8]. ***Statistical analysis:*** *Set#1 only:* For Set #1, the accuracy of segmentation algorithm was evaluated using (A) Dice coefficient = $2|Seg \cap GT|/(|Seg| \cup |GT|)$. (B) Spearman correlation coefficient (ρ). (C) Absolute volume difference (AVD). (D) Variability, $Var=|Seg-GT|/(0.5*(Seg+GT))$. *Pooled Data:* Next we pooled the data from Set#1 and Set#2 to determine any differences between PWI lesion segmentation with different quantitative maps. This was evaluated by using repeated measures ANOVA. Similar analysis was performed for mismatch calculations based on lesion segmentation with different maps. Statistical analyses performed using MedCalc®(v. 10.4).

Table 1	ρ - PWI lesion			ρ - Mismatch		
Set #1 only *(N = 25)*	MTT	T_{max}	TTP	MTT	T_{max}	TTP
GT	0.9	0.88	0.88	0.88	0.8	0.77

Table 1. Spearman correlation of GT PWI lesion with lesion segmentation on respective maps and corresponding mismatch calculation.

Table 2 *(N = 25)*	PWI lesion			Mismatch on respective maps		
	MTT (cc)	T_{max} (cc)	TTP (cc)	MTT (cc)	T_{max} (cc)	TTP (cc)
GT	40±37	52±41	51±41	41±44	53±45	53±47

Table 2. Absolute volume difference between GT and respective lesion segmentation(s) and corresponding mismatch volumes

Table 3 *(N = 25)*	PWI lesion segmentation					Mismatch on respective maps				
	Volume (cc)				Var (%)	Volume (cc)				Var (%)
	GT	MTT	T_{max}	TTP	MTT	GT	MTT	T_{max}	TTP	MTT
Mean	183	165	155	150	38	138	113	108	102	38
IQR	77- 242	66- 255	60- 238	62-200	10 - 37	60 - 205	50 – 171	44 - 174	27- 146	14 - 72

Table 3. Overall comparative statistics on GT marked PWI lesion and those obtained from automated segmentation on respective maps, along with corresponding mismatch.

Results & Discussion: We observed a strong correlation (ρ = 0.9) between GT PWI lesion volume and MTT based automated PWI lesion segmentation volume (Table 1), consistent with those reported previously for using supervised lesion segmentation method [3]. Clustering of segmented islands integrated with feedback from island statistics provides reliable segmentation, which along with ventricle removal, enables to correctly identify the lesion as defined in clinical setting (Fig. 1). Overall, the processing time, from map generation to MM calculation varied from 30 s (25 phases, 64 x 64 matrix) to 150 s (100 phases, 128 x 128 matrix). The median Dice value of 0.74 indicated a good overlap between GT PWI lesion and MTT based automated PWI lesion segmentation. For MTT based mismatch calculation, ρ of 0.88, though lower compared to manually segmented inter-rater correlation (ρ =0.96) [8], is consistent with those reported for automated mismatch techniques [4]. For MTT based PWI lesion segmentation, the mean absolute difference (40±37 cc) was twice that reported with manually segmented volumes (19±34 cc[9]). Variability metric, which normalized any size effect, showed that variability on manually done GT (83%±79%) was greater than with automated PWI lesion segmentation on MTT maps (38%±52%) (Table 3). However for MM, both the AVD (41±44 cc) and the variability (38%±32%[9]) were higher for automated segmentation compared to manually segmented volumes (25%±90%[8]). For Set#1, repeated measures ANOVA showed no differences between the GT and PWI lesion segmentation with MTT, TTP and T_{max} maps. Similar effect was observed for respective mismatch calculation. Repeated measures ANOVA with pooled data (N = 84) revealed that mean lesion volume obtained from T_{max} maps (173 cc) was lower (p = 0.03) compared to those obtained using MTT maps (188 cc) (Fig. 2), consistent with earlier findings in AIS [2]. Possible sources of discrepancies between automated PWI lesion segmentation and GT include: (a) Inability to mark the entire affected vascular territory as infarcted, suggesting the need to incorporate clinical knowledge in segmentation and (b). Failure of difference threshold calculation due to improper skull removal. The current algorithm considers each map independently and combining information from different maps can further improve the performance of the algorithm.

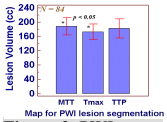

Figure 2. PWI lesions segmented on Tmax based maps have lower volumes, compared to MTT map based lesions.

Conclusions: A fully automated PWI lesion segmentation and mismatch calculation algorithm is feasible, offering robust segmentation on different quantitative PWI maps and improves on current state-of-the art algorithms.

References: [1] Ann. Neuro.2006, 60:508-517 [2] Stroke 2005; 36:1153-1159. [3] Comp.Biol.Med. 2006; 36:1268-1287. [4] ISMRM Proc.2009; Vol. 17, pg. 728. [5] ISMRM Proc. 2009; Vol. 17, pg. 4710. [6] MRM 2003;50:164-174. [7] http://www.itk.org. [8] AJNR, 2007; 28:1674-78. [9] Stroke. 2006; 37:2951-2956.